(7) Smith, T. E.; Carpenter, D. K. *Macromolecules* **1968**, *1*, 204.
(8) Fujita, H. *Polym. J.* **1970**, *1*, 537.
(9) Noda, I.; Imai, M.; Kitano, T.; Nagasawa, M. *Macromolecules* **1983**, *16*, 425.
(10) Matsushita, Y.; Furuhashi, H.; Choshi, H.; Noda, I.; Nagasawa, M.; Fujimoto, T.; Han, C. C. *Polym. J.* **1982**, *14*, 489.
(11) Ohtani, H.; Tsuge, S.; Matsushita, Y.; Nagasawa, M. *Polym. J.* **1982**, *14*, 493.
(12) Glinka, C. J. *AIP Conf. Proc.* **1981**, *No. 89*, 395–397.
(13) Amis, E. J.; Glinka, C. J.; Han, C. C.; Hasegawa, H.; Hashimoto, T.; Lodge, T. P.; Matsushita, Y. *Polym. Prepr., Am. Chem. Soc., Div. Polym. Chem.* **1983**, *2442*, 215.
(14) Duplessix, R.; Cotton, J. P.; Benoit, H.; Picot, C. *Polymer* **1979**, *20*, 1181.
(15) Ohta, T.; Oono, Y.; Freed, K. F. *Macromolecules* **1981**, *14*, 1588.
(16) Cotton, J. P.; Decker, D.; Benoit, H.; Farnoux, B.; Higgins, J.; Jannink, G.; Ober, R.; Picot, C.; des Cloizeaux, J. *Macromolecules* **1974**, *7*, 863.
(17) Berry, G. C. *J. Chem. Phys.* **1966**, *44*, 4550.
(18) Yamamoto, A.; Fujii, M.; Tanaka, G.; Yamakawa, H. *Polym. J.* **1971**, *2*, 799.
(19) Fukuda, M.; Fukutomi, M.; Kato, Y.; Hashimoto, T. *J. Polym. Sci., Polym. Phys. Ed.* **1974**, *12*, 871.
(20) Kurata, M.; Yamakawa, H.; Teramoto, E. *J. Chem. Phys.* **1958**, *28*, 785.
(21) Wall, F. T.; Erpenbeck, J. J. *J. Chem. Phys.* **1959**, *30*, 634.
(22) Alexandrowicz, Z.; Accad, Y. *J. Chem. Phys.* **1971**, *54*, 5338.
(23) Barrett, A. J. *Macromolecules*, submitted.
(24) des Cloizeaux, J. *J. Phys.* **1980**, *41*, 223.
(25) Oono, Y.; Ohta, T. *Phys. Lett. A* **1981**, *85A*, 480.
(26) Farnoux, B.; Boue, F.; Cotton, J. P.; Daoud, M.; Jannink, G.; Nierlich, M.; de Gennes, P.-G. *J. Phys. (Paris)* **1978**, *39*, 77.
(27) Disclaimer: Certain commercial materials and equipment are identified in this paper in order to specify adequately the experimental procedure. In no case does such identification imply recommendation or endorsement by the National Bureau of Standards nor does it imply that the material or equipment identified is necessarily the best available for this purpose.

Electron Paramagnetic Resonance Studies of Amine-Cured Epoxy Resins: Dependence of Nitroxide Spin-Probe Mobility on Cross-Link Density, Free Volume, and Temperature

T. C. Sandreczki* and I. M. Brown

McDonnell Douglas Research Laboratories, St. Louis, Missouri 63166.
Received December 29, 1983

ABSTRACT: Studies were made of the electron paramagnetic resonance line shapes of the nitroxide spin probes TANOL and TEMPENE in amine-cured epoxy resin matrices above their glass transition temperatures. The rotational correlation times deduced from these line shapes were measured as a function of temperature and matrix cross-link density. Fractional free volumes, glass transition temperatures, and cross-link densities of the matrices were determined by linear expansion measurements, differential scanning calorimetry, and dynamic mechanical analysis and/or sample stoichiometry, respectively. The rotational correlation times were dependent on the fractional free volume and temperature. The dependence on the free volume was in the form of a modified WLF equation and yielded values of $\sim$0.4 for the Doolittle parameter. The explicit temperature dependence had an Arrhenius form with a preexponential factor of $\sim 10^{-12}$ s and an activation energy of $\sim$19 kJ mol^{-1}. At a constant temperature the logarithm of the rotational correlation time was a linear function of matrix cross-link density. This relationship appears to be a direct consequence of the linear dependence of the glass transition temperature on cross-link density.

Introduction

Amine-cured epoxy resins are thermosetting polymers that are widely used in the aerospace industry as matrix materials for fiber-reinforced composite structural components. Molecular mobility and the associated free volume are important parameters in such thermosetting polymers since they can determine mechanical and transport properties and the value of the glass transition temperature. In this study we have used the techniques of dynamic mechanical analysis (DMA), thermomechanical analysis (TMA) (linear expansion measurement), differential scanning calorimetry (DSC), and electron paramagnetic resonance (EPR) spectroscopy to investigate the dependence of molecular mobility on temperature and cross-link density for a series of chemically similar amine-cured epoxy resin polymers. In the EPR experiments the spin-probe method was used. This technique entails the use of stable nitroxide free radicals as probes of their dynamic environments in the polymer network.

Experimental Section

Materials. The samples investigated were prepared from the diglycidyl ether of bisphenol A (DGEBA) epoxy in the form of the DER 332 commercial resin obtained from Dow Chemical Co. This resin had a nominal average equivalent weight of 172–176 compared with 170 for pure DGEBA monomer, indicating that small amounts of higher order oligomers were present.

The aliphatic amine curing agents *N,N'*-dimethyl-1,6-diaminohexane (DDH) and 1,4-diaminobutane (DAB) obtained from Aldrich Chemical Co. had ≥97%

The nitroxide spin probes 4-hydroxy-2,2,6,6-tetramethylpiperidine-1-oxyl (TANOL) and 2,2,6,6-tetramethyl-1,2,3,6-tetrahydropyridine-1-oxyl (TEMPENE) were obtained from Eastman Kodak Co. and Molecular Probes, respectively. All materials were used as received. Their chemical structures are shown in Figure 1.

Sample Preparation. Amine-cured epoxy samples having different average cross-link densities were prepared by using mixtures of the tetrafunctional amine DAB and the difunctional amine DDH. The samples contained the following ratios (by equivalents) of DAB:DDH:DGEBA: 0:5:5, 2:3:5, 3:2:5, and 5:0:5. The amines were first mixed in the desired ratios and then added to a stoichiometric amount of DGEBA containing less than 0.03 wt % nitroxide. EPR, DSC, and TMA samples were cast in glass tubes. Separately prepared DMA samples were cast in silicone rubber molds. All samples were cured for at least 15 h at room temperature followed by postcuring above the glass transition temperature, T_g.

Measurements. Torsional dynamic mechanical measurements were made with a Rheometrics dynamic spectrometer (Model RDS

0024-9297/84/2217-1789$01.50/0

Table I
Values of Parameters Used in the Calculation of Sample Cross-Link Densities

sample (DAB:DDH:DGEBA)	G', Pa	T, K	ρ, kg/L	ν, mol/L	M from G'	M from eq 2
0:5:5			1.12			
2:3:5	5.0×10^6	383	1.13	0.83	1370	1135
3:2:5	6.6×10^6	401	1.14	1.0	1090	720
5:0:5	1.9×10^7	443	1.16	2.7	425	390

Resin

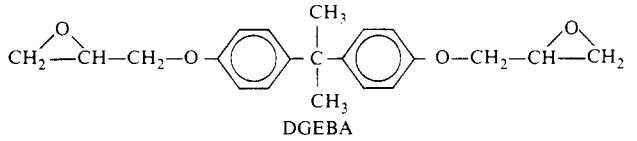

DGEBA

Curing agents

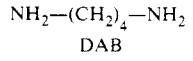

DAB

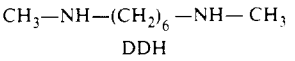

DDH

Spin probes

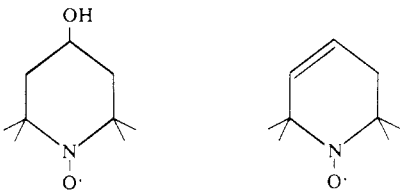

TANOL TEMPENE

Figure 1. Chemical structures of materials employed in this study.

7700). Samples having dimensions 6 × 1.2 × 0.3 cm were examined at a frequency of 1.6 Hz over a temperature range from 298 K to above T_g.

Sample glass transition temperatures were determined by DSC using a DuPont thermal analyzer (Model 990), DSC cell, and cell base. Samples were heated at a rate of 10 K min^{-1} from 50 K below T_g to 50 K above T_g. Sub-T_g annealing effects were eliminated by quenching the samples from above T_g before the DSC measurement.

Volume expansion coefficients were derived from linear expansion coefficients determined with a DuPont thermomechanical analyzer (Model 942) interfaced with a microprocessor-controlled DuPont thermal analyzer (Model 1090). Measurements were made from 50 K below T_g to 50 K above T_g at a rate of 10 K min^{-1}.

The EPR spectrometer employed was a Varian X-band instrument (Model E-102 Century Series) interfaced to a Varian data acquisition system (Model E-900).

Results

Cross-link densities were determined for the different stoichiometric samples from the results of the torsional dynamic mechanical measurements. Values of the dynamic shear storage modulus, G', measured as a function of temperature are shown in Figure 2. The cross-link densities were calculated from the plateau region above T_g with the following equation derived from the theory of rubber elasticity:

$$G' = \alpha\nu RT = \alpha\frac{\rho RT}{M} \tag{1}$$

where ν is moles of cross-links per m^3 of sample, R is the gas constant, T is degrees K, α is a front factor with a value ~1.88 for aliphatic amine-cured epoxies,[1] ρ is the sample density, and M is the average molecular weight between cross-links.

The measured cross-link densities and molecular weights between cross-links are shown in Table I. Also shown in

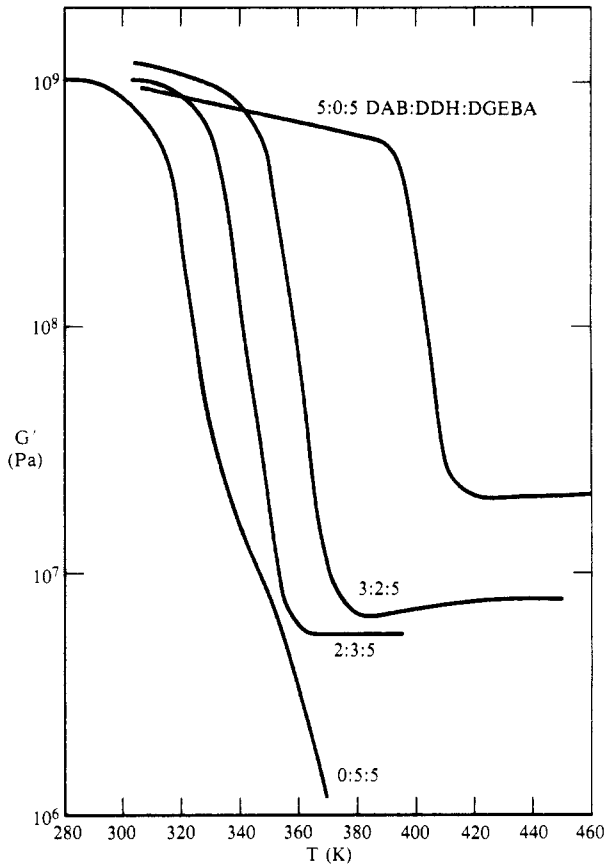

Figure 2. Shear modulus, G', as a function of temperature for the amine-cured samples of DGEBA having the stoichiometries indicated.

Table I are the theoretical values of M evaluated from the curing agent stoichiometry with the equation

$$M = \frac{2}{f}\left(\frac{w}{m}\right) \tag{2}$$

where f depends on the functionality of the amine (e.g., $f = 4$ for DAB or $f = 0$ for DDH), m is the number of moles of DAB in the sample, and w is the sample weight. The experimental and theoretical values of M shown in Table I are in reasonable agreement. The cross-link density of the 0:5:5 sample could not be measured by DMA; however, swelling experiments with methylene chloride indicated that the cross-link density was ~0.3 of that of the 2:3:5 sample.

The T_g values were determined from the DSC scans and were defined as the temperatures at the inflection points of the glass transitions. T_g values also were determined from DMA for comparison with the DSC results and were defined as the temperatures at which the maxima in the tangents of the loss angles (i.e., G''/G', where G'' is the dynamic loss modulus) occurred. The T_g values are listed in Table II and are plotted as a function of M^{-1} in Figure 3, where M is determined from either eq 1 or eq 2. The T_g values determined from DMA data were slightly higher than those obtained from the DSC data. This difference

Table II
Glass Transition Temperatures, Expansion Coefficients, and Values of Temperatures and Free Volumes at $\tau_c = 10^{-9}$ and 10^{-10} s

sample	T_g, K (DSC)	$\alpha \times 10^4$	$T - T_g$ at $\tau_c = 10^{-9}$ s	$T - T_g$ at $\tau_c = 10^{-10}$ s	$f(\tau_c = 10^{-9}$ s)[a]	$f(\tau_c = 10^{-10}$ s)[a]
0:5:5	301	4.4	83	128	0.062	0.081
2:3:5	330	4.0	83	135	0.058	0.079
3:2:5	347	3.6	85	134	0.056	0.073
5:0:5	398	3.1	82	~136	0.050	0.067

[a] Assuming f at $T_g = 0.025$ for each sample.

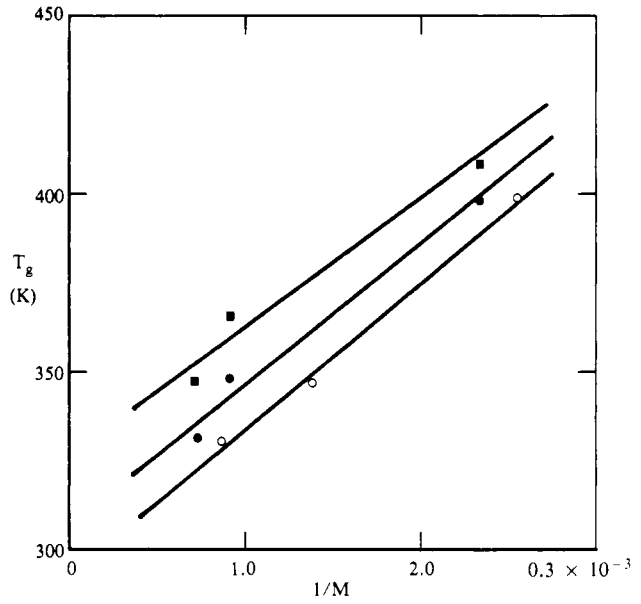

Figure 3. T_g values of DMA and EPR samples plotted vs. M^{-1}. Samples: (■) DMA samples with T_g measured by DMA; (●) DMA samples with T_g measured by DSC; (○) EPR samples with T_g measured by DSC.

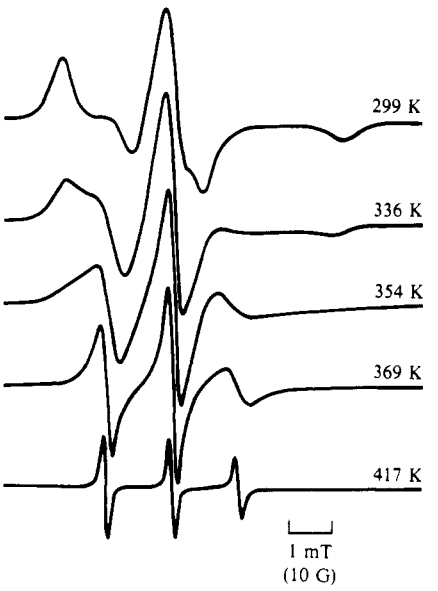

Figure 4. Temperature dependence of EPR spectra of TANOL in 0:5:5 DAB:DDH:DGEBA.

is probably the result of the difference in the characteristic frequencies of the techniques employed (1.6 Hz for DMA and ≤ 0.1 Hz for DSC). The data shown in Figure 3 show a reasonable fit to the form

$$T_g = T_{g0} + C/M \tag{3}$$

where T_{g0} is the T_g value of the un-cross-linked polymer and C is an empirical parameter. The solid lines in Figure 3 give the values $C = 4 \times 10^4$ K, which compares favorably with the value given by Nielsen[2] ($C = 3.9 \times 10^4$ K).

Fractional free volumes, $f(T)$, were determined at several temperatures from the thermal expansion data by using the expression

$$f(T) = f(T_g) + \alpha(T - T_g) \tag{4}$$

where $f(T_g)$ is the fractional free volume at $T = T_g$ and α is the difference in thermal expansion coefficients above and below T_g. The values of α decreased with increasing cross-link density and are listed in Table II.

The EPR spectra for TANOL and TEMPENE in the amine-cured epoxy samples were recorded at different temperatures from below room temperature to 135 K above T_g. Typical examples of the observed spectra are shown in Figure 4. With increasing temperature all the spectra exhibited typical features indicating the onset of motional collapse and line narrowing. At all temperatures, each spectrum could be characterized by essentially one value of the motional correlation time or, at most, by a narrow distribution of correlation times. For temperatures below T_g it was clear from the line shapes of both nitroxides that the motional correlation times were longer than 3×10^{-9} s and increased with decreasing temperature.

Using current slow-motion theories in the form of computer simulations[3] of the observed line shapes or analytic techniques[4] based on computer simulations, it is possible to determine the absolute values of sub-T_g motional correlation times to an order-of-magnitude estimate. Since the large numbers of parameters determining the overall line shape make unique fits of the computer simulations to the observed line shapes difficult, we chose only to compare qualitatively the sub-T_g correlation times.

At temperatures above $T_g + 20$ K the observed spectra consisted of three motionally narrowed lines. By employing the theory of Kivelson[5] we calculated the values of τ_c from the spectral amplitudes and line widths. The equation used for $\tau_c \leq 3 \times 10^{-9}$ s was

$$\tau_c = 4\left[\left(\frac{Y(0)}{Y(1)}\right)^{1/2} + \left(\frac{Y(0)}{Y(-1)}\right)^{1/2} - 2\right] b^{-2} W(0)^{-1} \tag{5a}$$

with

$$b = \frac{4\pi}{3}\left[A_{zz} - \frac{1}{2}(A_{xx} + A_{yy})\right] \tag{5b}$$

where $Y(1)$, $Y(0)$, and $Y(-1)$ are the amplitudes of the low-, middle-, and high-field lines, respectively. A_{xx}, A_{yy}, and A_{zz} are the principal components of the nitrogen hyperfine tensor, and $W(0)$ is the line width of the center line. The values $A_{zz} = 97$ MHz (3.45 mT) and $A_{xx} = A_{yy} = 17$ MHz (0.6 mT) were used for TANOL and the values $A_{zz} = 98$ MHz (3.5 mT) and $A_{xx} = A_{yy} = 17$ MHz (0.6 mT) were used for TEMPENE.

Values of τ_c are plotted on a logarithmic scale as a function of reciprocal temperature in Figures 5 and 6 for TANOL and TEMPENE, respectively. All the plots are approximately linear for the values $\tau_c \leq 10^{-9}$ s. Also, as

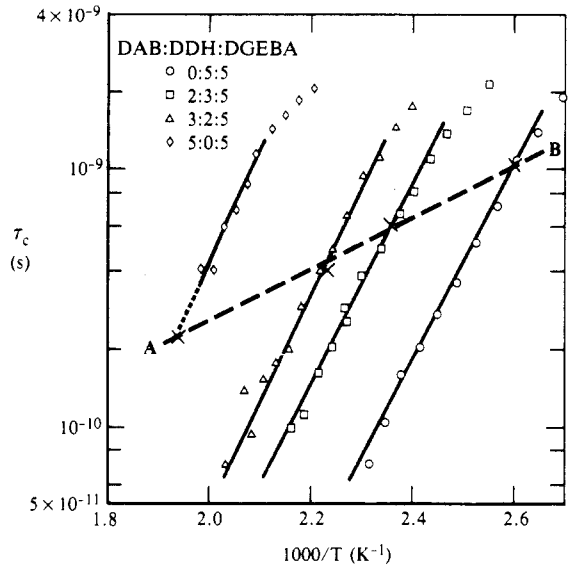

Figure 5. Temperature dependence of motional correlation times for TANOL in samples of amine-cured DGEBA with different cross-link densities. Points marked "×" have fractional free volumes of 0.062.

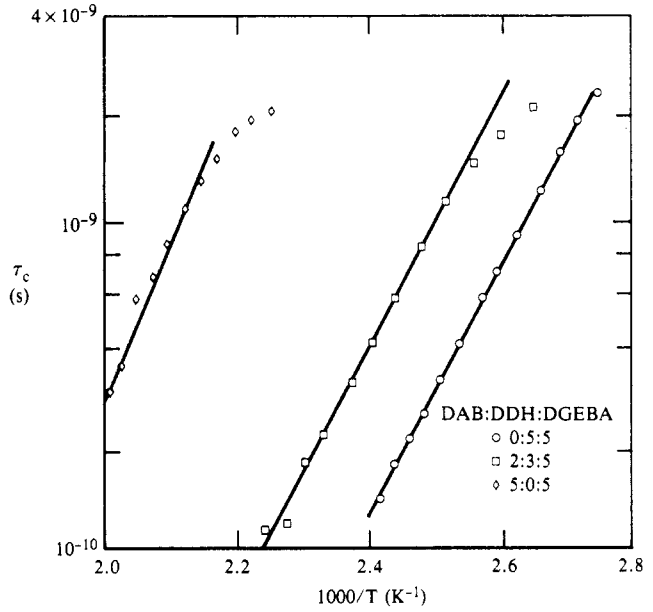

Figure 6. Temperature dependence of motional correlation times for TEMPENE in samples of amine-cured DGEBA with different cross-link densities.

is shown in Figure 7 for TANOL data at 417, 435, and 463 K, log (τ_c) increases linearly with cross-link density calculated from eq 2. The linearity of the plots in Figure 7 is a consequence of (1) the plots in Figures 5 and 6 being nearly parallel, (2) the intercepts being nearly linearly dependent on T_g, and (3) (as shown in Figure 3) T_g varying linearly with cross-link density. The linear dependence of the intercepts on T_g can be seen by comparing the temperatures at which τ_c for TANOL in the different samples has a particular value. Thus, as shown in Table II, for each sample $\tau_c = 10^{-9}$ s occurs at (T_g + (84 ± 2 K)) and $\tau_c = 10^{-10}$ s occurs at (T_g + (133 ± 5 K)). Similar observations were made in the samples containing TEMPENE.

The linearity of the plots in Figures 5 and 6 for $\tau_c \leq 10^{-9}$ s implies that the motional frequency (i.e., $1/2\pi\tau_c$) follows an apparent Arrhenius temperature dependence, viz.

$$\tau_c = \tau_{c0} \exp(\Delta E/RT) \quad (6)$$

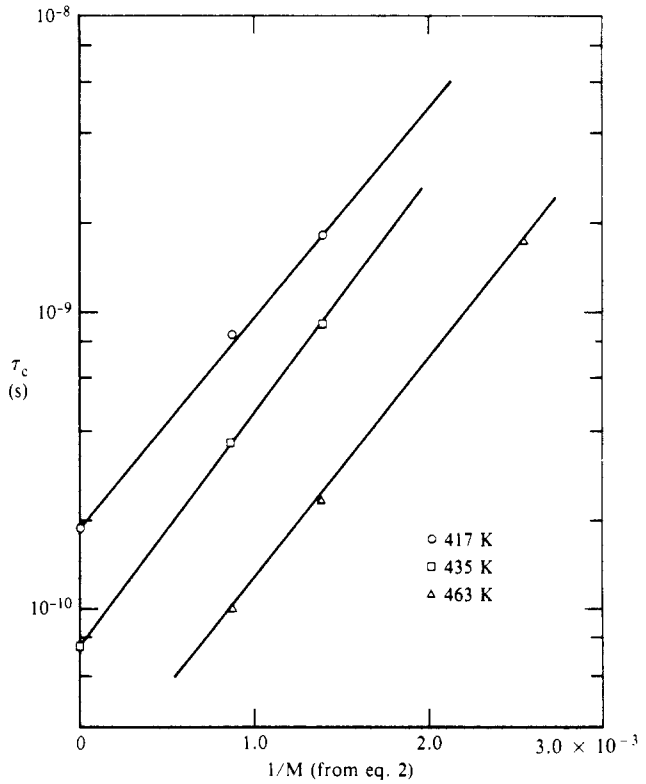

Figure 7. Correlation times at the selected temperatures shown for TANOL in samples having different molecular weights between the cross-links.

where τ_{c0} is the preexponential factor and ΔE is the activation energy for the rotational motion of the spin probe. Typical values of $\tau_{c0} = 10^{-20}$ s and $\Delta E \simeq 50$ kJ mol^{-1} were obtained from the data. Since the former value has no physical meaning for times shorter than $\tau_{c0} \simeq 10^{-13}$ s,[6] it seems unlikely that the observed temperature dependence of τ_c follows true Arrhenius behavior, i.e., that the observed activation energy corresponds to a physical barrier height. Thus, the observed temperature dependence of the spin-probe motion is not described exclusively by the Arrhenius equation. In fact, as we shall show, above T_g of the host polymer the motional correlation time of the spin probe depends primarily on the fractional free volume of the polymer.

From Figures 5 and 6 and the results in Table II, it appears that above T_g the logarithms of the rotational correlation times for both TANOL and TEMPENE in the epoxy samples show a linear dependence on the difference between the sample temperature and the polymer T_g value. This observed linear dependence of log (τ_c) vs. ($T - T_g$) suggests the modified form of the WLF equation,[6,7] viz.

$$-1/\ln(\tau_c/\tau_{cR}) = f_R^2/[B\alpha(T - T_R)] + f_R/B \quad (7)$$

where τ_c and τ_{cR} are the motional correlation times of the spin probe at temperature T and reference temperature T_R, f_R is the free volume fraction at T_R, B (≈0.4–0.6) is the coefficient that appears in the Doolittle equation,[8] and α is the difference in the thermal expansion coefficients above and below T_g. Typical plots of $-1/\ln(\tau_c/\tau_{cR})$ vs. $1/(T - T_R)$ for TANOL and TEMPENE are shown in Figures 8 and 9. In these plots, τ_{cR} equals 10^{-9} s and T_R equals 385 and 379 K, respectively. The linearity indicates that eq 7 is apparently obeyed by both nitroxides in all the amine-cured epoxides studied. This agreement of the data with eq 7, which is based on free volume, implies that above T_g the τ_c values for the spin probes depend on the fractional free volume in the host polymer.

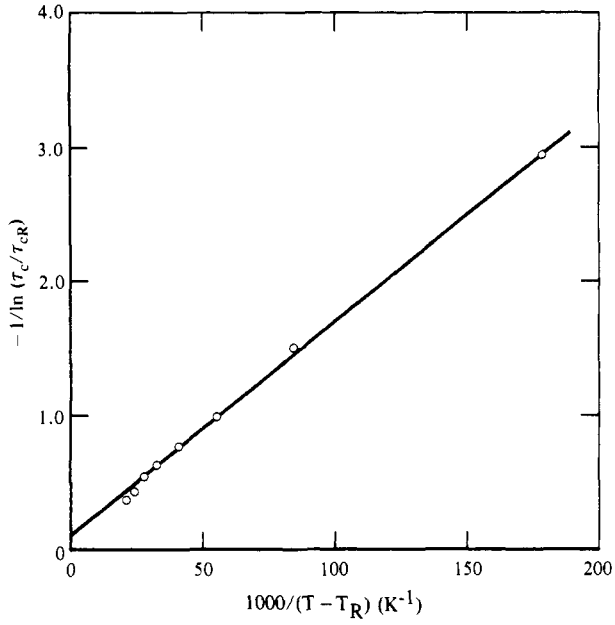

Figure 8. WLF plot for TANOL in 0:5:5 DAB:DDH:DGEBA.

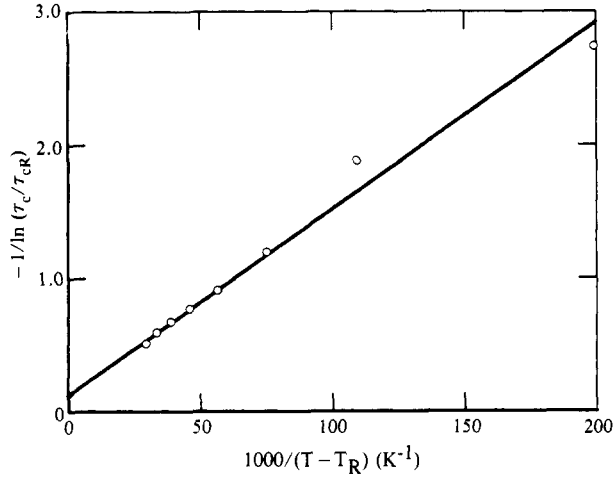

Figure 9. WLF plot for TEMPENE in 0:5:5 DAB:DDH:DGEBA.

It would be incorrect, however, to conclude that τ_c depends exclusively on sample free volume, since the spectral line shapes (and therefore τ_c values) change with temperature even below T_g, where the free volume of a sample is considered to be constant. We can therefore reasonably assume that above T_g there is an explicit dependence of the motional correlation times of the spin probe on absolute temperature in addition to the temperature dependence implied in the modified WLF equation. The following evidence further supports this contention. It can be seen from Table II that the thermal expansion coefficients are different for samples with different cross-link densities. As a result, if one uses eq 4 and assumes that the free volumes in all samples are the same at T_g, then it follows that the free volumes corresponding to a TANOL correlation time of $\tau_c = 10^{-9}$ s (i.e., occurring at $T = T_g + (83 \pm 2$ K)) are different in samples having different cross-link densities. The same conclusion can be drawn for the free volumes corresponding to $\tau_c = 10^{-10}$ s (see Table II).

There is evidence from our EPR studies supporting the assumption that the free volume at or below T_g is the same or nearly the same in these samples: The EPR line shapes (and hence the correlation times) are the same for all but one of the samples at a common temperature (e.g., 295 ± 2 K) that is below the T_g of the 0:5:5 sample. The one exception is the 0:5:5 sample, which must be maintained at 15 K below the common temperature, to produce the same line shape as the other samples. This corresponds to a difference in fractional free volume of about 0.001, which is sufficiently small to be considered negligible for our purposes.

Above T_g when the temperature is adjusted to make the calculated values of free volume equal in the different samples, the motional correlation times of the 0:5:5 and the 5:0:5 samples differ by approximately an order of magnitude. This result is illustrated in Figure 5, where line AB is a calculated "iso-free volume" line drawn through points, marked "×", at which each of the samples is calculated to have a fractional free volume of 0.062. (A fractional free volume of 0.025 was assumed in all samples at $T = T_g$.) Line AB can be considered as the temperature dependence of τ_c in a sample maintained, by appropriate adjustment of cross-link density, at a constant free volume value of 0.062. Thus, line AB describes the Arrhenius contribution to the temperature dependence of τ_c. An activation energy of 19 kJ mol^{-1} was evaluated from the slope of line AB. This value is somewhat larger than the values reported[9] below T_g (4–8 kJ mol^{-1}) but significantly smaller than the value of ~50 kJ mol^{-1} obtained from the slopes of the lines in Figures 5 and 6. Furthermore, the preexponential factor τ_{c0} for line AB is $\sim 10^{-12}$ s, which is a physically meaningful value.

It is clear that the temperature dependence of τ_c at constant free volume (as depicted by line AB for the 0:5:5 sample) does not account for the total change in correlation time with temperature. For example, at 429 K, where the actual τ_c value is 10^{-10} s for the 0:5:5 sample, the value of τ_c on line AB is 5.5×10^{-10} s. Thus, the increase in spin-probe motion solely attributable to the Arrhenius temperature dependence in this sample accounts for only 25% of the change in log (τ_c) when τ_c actually changes from 10^{-9} to 10^{-10} s. The rest of the change in τ_c with temperature is assigned to free volume changes in the sample. In this case, the change in τ_c from 5.5×10^{-10} to 10^{-10} s at 429 K is associated with the sample free volume changing from 0.062 to 0.081. The τ_c data for the other samples were analyzed in the same way.

To quantitatively describe the above results for the rotational correlation time of the nitroxide spin probes, we use an expression that explicitly includes both free volume and temperature as the independent variables controlling τ_c. This expression is analogous to one describing the temperature dependence of translational diffusion[10,11] and can be written in the following form:

$$\ln \frac{\tau_c}{\tau_{cR}} = \ln \frac{\tau_c}{\tau_{cR'}} + \ln \frac{\tau_{cR'}}{\tau_{cR}} \tag{8}$$

with

$$\ln \frac{\tau_c}{\tau_{cR'}} = B\left(\frac{1}{f} - \frac{1}{f_R}\right) \tag{8a}$$

and

$$\ln \frac{\tau_{cR'}}{\tau_{cR}} = \frac{\Delta E}{R}\left(\frac{1}{T} - \frac{1}{T_R}\right) \tag{8b}$$

where τ_c is the rotational correlation time of the spin probe at temperature T and free volume f calculated from eq 4 assuming $f(T_g) = 0.025$, τ_{cR} is the corresponding value of τ_c at T_R and f_R, the reference temperature and free volume, respectively, and $\tau_{cR'}$ is the value of τ_c at T and f_R. The free volume term in eq 8a is written in the form of the Doolittle equation,[8] from which the WLF equation can be

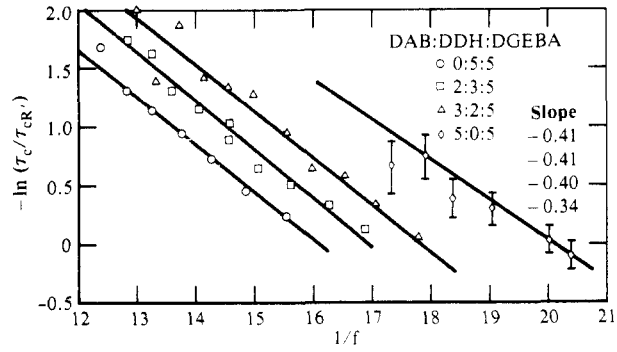

Figure 10. Plots of $-\ln(\tau_c/\tau_{cR'})$ vs. $1/f$ for TANOL in samples of different cross-link density.

derived. The term in eq 8b expresses the explicit temperature dependence and accounts for the observed Arrhenius contribution to τ_c.

Plots of $\ln(\tau_c/\tau_{cR'})$ vs. $1/f$ are shown in Figure 10. Values of $\tau_{cR'}$ and τ_c for the 0:5:5 sample at any temperature were evaluated from the correlation time on line AB and the actual correlation time, respectively, at that temperature. For example, at 429 K, $\tau_{cR'}$ equals 5.5×10^{-10} s and τ_c equals 1.0×10^{-10} s. The corresponding values for the other samples were determined in the same way. It is clear from the linearity of the plots that the motional correlation times after removal of the Arrhenius contribution follows eq 8a. The slopes of these lines are equal to $-B$, the Doolittle parameter. Although there is a large scatter in the data for the 5:0:5 sample, for all samples $B \approx 0.4$ rather than $B \approx 1.0$ as is the case for translational diffusion. This smaller value of B indicates that the rotational diffusion rates are less sensitive to free volume than are the translational diffusion rates. This result is not surprising since translational diffusion requires "free volume holes" approximately the diameter of the diffusing molecule whereas rotational diffusion requires much smaller "free volume holes".[12]

The value of $f(T_g)$ used in calculating f for all samples in Figure 10 was 0.025. Changes in $f(T_g)$ from 0.025 to either 0.030 or 0.020 result in changes in the value of B from 0.4 to 0.45 or 0.35, respectively. Thus, the value of B obtained from Figure 10 ($B \approx 0.4$) is not strongly dependent on the assumed value of $f(T_g)$.

The data in Figure 10 can be replotted in the form suggesting the WLF equation, eq 7. Typical results are shown for TANOL in the 0:5:5 sample in Figure 11, where the reference values for the temperature and correlation time were taken from the intercept of the corresponding line in Figure 10 with the X-axis (i.e., $\tau_c = \tau_{cR'}$). The linearity of the plot in Figure 11 indicates that the motional correlation times still obey the WLF equation even after a correction has been made for the contribution from the Arrhenius temperature dependence.

Conclusions

The values of the rotational correlation times for the two spin probes TANOL and TEMPENE in amine-cured epoxy resin polymers with different cross-link densities above T_g can be fitted to either (1) an Arrhenius temperature dependence with an activation energy of $\sim$50 kJ mol^{-1} and a frequency factor of $\sim 10^{-20}$ s or (2) a modified form of the WLF equation. The former dependence can be disregarded since the frequency factors are physically unreal. The latter dependence implies that the τ_c values depend on the amount of free volume present in the host polymers above T_g. However, when the temperature dependences

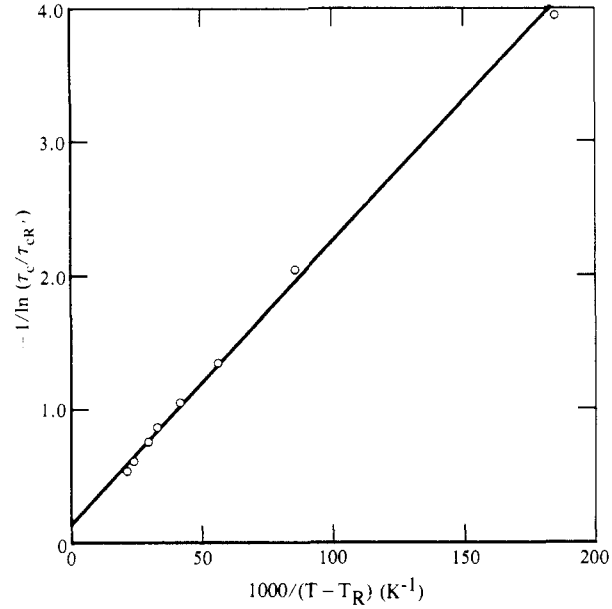

Figure 11. Corrected WLF plot for 0:5:5 sample from data in Figure 10.

are corrected for the free volume contents, there still remains an Arrhenius temperature dependence with a preexponential factor of 10^{-12} s and an activation energy of $\sim$19 kJ mol^{-1}.

The logarithms of the rotational correlation times are also linearly dependent on cross-link density evaluated from the dynamic shear modulus. This relation is a direct consequence of the linear dependence of T_g on the cross-link density.

As a general conclusion, we have shown that the EPR data obtained with nitroxide spin probes can be correlated with DMA, DSC, and TMA data. In so doing, we have demonstrated that the spin-probe method can be considered as an additional technique to provide useful information about amine-cured epoxy polymers above T_g.

Acknowledgment. This research was conducted in part under the McDonnell Douglas Corp. Independent Research and Development Program and in part under Naval Air Systems Command Contract N00019-80-C-0552. We gratefully acknowledge discussions with D. P. Ames and A. C. Lind.

Registry No. DER 332, 25085-99-8; DDH, 13093-04-4; DAB, 110-60-1; TANOL, 2226-96-2; TEMPENE, 3264-93-5.

References and Notes

(1) Katz, D.; Tobolsky, A. V. *Polymer* **1963**, *4*, 417.
(2) Nielsen, L. E. "Mechanical Properties of Polymers and Composites"; Marcel Dekker: New York, 1974; Vol. 1.
(3) Freed, J. H.; Bruno, G. V.; Polnaszek, C. F. *J. Phys. Chem.* **1971**, *75*, 3385.
(4) Goldman, S. A.; Bruno, G. V.; Freed, J. H. *J. Phys. Chem.* **1972**, *76*, 1858.
(5) Kivelson, D. *J. Chem. Phys.* **1960**, *33*, 1094.
(6) Buchachenko, A. L.; Kovarskii, A. L.; Vasserman, A. M., In "Advances in Polymer Science"; Rogovin, Z. A., Ed.; Halsted Press: New York, 1974.
(7) Williams, M. L.; Landel, R. F.; Ferry, J. D. *J. Am. Chem. Soc.* **1955**, *77*, 3701.
(8) Doolittle, A. K. *J. Appl. Phys.* **1951**, *22*, 1471.
(9) Kovarskii, A. L.; Plaček, J.; Szöcs, F. *Polymer* **1978**, *19*, 1137.
(10) Macedo, P. B.; Litovitz, T. A. *J. Chem. Phys.* **1965**, *42*, 245.
(11) Chung, H. S. *J. Chem. Phys.* **1966**, *44*, 1362.
(12) Kovarskii, A. L.; Wasserman, A. M.; Buchachenko, A. L., In "Molecular Motion in Polymers by ESR"; Boyer, R. F., Keinath, S. E., Eds.; Harwood Academic Publishers: New York, 1980.